On the Relation between the used Organic Sulphur Salts and the Properties of Cadmium Sulphide Nanocrystals

Eman M. Ismael[1], Hassan M. Salman[1], Ahmed. M. Abo-Bakr[1], A. A. Ebnalwaled [2]

[1] Department of Chemistry, South Valley University, Qena 83523, Egypt.

[2] Electronics and Nano Devices Lab, Physics Department, Faculty of Science, South Valley University, Qena, 83523 Egypt.

Abstract:- In this study, we synthesized three distinct CdS nanocrystals through a straightforward chemical method employing different organic sulphur salts, namely thiocarbonhydrizide, thiocarbonic acid dipotassium salt, and thiocarbonyl bis-thioglycolic acid. The synthesized nanocrystals underwent comprehensive characterization utilizing various analytical techniques, including transmission electron microscopy, FT-IR spectroscopy, H1-NMR spectroscopy, Mass Spectra analysis, X-ray diffraction, and UV-vis spectrophotometry.

We identified crucial characteristics, including production efficiency, elemental makeup, lattice dimensions, crystallite dimensions, microstructural distortions, light transmittance, light absorption, and energy band gap, for each of the synthesized CdS nanocrystals. Our findings revealed crystal sizes of 22.56 nm, 12.70 nm, and 4.65 nm, as well as energy band gaps of 4.87 eV, 3.22 eV, and 5.03 eV for the CdS (I), CdS (II), and CdS (III) samples, respectively.

Keywords:- *CdS nanocrystals, Organic Sulphur Sources, Optical Properties, Lattice Parameters.*

I. INTRODUCTION

The synthesis of metal sulphide nanoparticles, with a particular emphasis on cadmium sulphide (CdS) nanocrystals, has garnered substantial attention within the dynamic field of nanomaterial research [1-5]. The strategic use of salt forms derived from simple organic sulphur compounds in nanoparticle synthesis has emerged as a pivotal facet in this research domain, offering a promising avenue for the precise tailoring of properties and characteristics exhibited by these nanocrystals [6-11].

Remarkably, the incorporation of these organic sulphur salts into the nanoparticle preparation process has consistently yielded nanocrystals characterized by exceptional attributes and well-defined properties. This intriguing phenomenon has captivated researchers worldwide, prompting them to delve deeper into the underlying mechanisms responsible for these favourable outcomes [12-18]. One prevailing hypothesis canters on the distinct kinetics governing organic reactions in contrast to their inorganic counterparts.

In comparison to the rapid and often uncontrollable kinetics associated with inorganic reactions, organic reactions tend to proceed at a more deliberate and controlled pace [19]. This temporal contrast in reaction rates presents a unique opportunity for researchers to exert precise control over critical aspects of the CdS nanocrystal formation process, including nucleation, growth, and surface chemistry [20-22]. Consequently, the incorporation of organic sulphur salts into the synthesis process represents a strategic choice, empowering researchers to tailor not only the size but moreover the resulting CdS nanocrystals' structure and optical characteristics [23].

Considering these compelling prospects, the present study embarks on a comprehensive exploration aimed at unravelling the intricate interplay between various organic sulphur salt precursors and the synthesis and properties of CdS nanocrystals. Leveraging a diverse array of cutting-edge characterization techniques and in-depth analyses [24, 25], we endeavour to elucidate the nuanced factors that underlie the rational design and optimization of CdS nanocrystals [26, 27].

Our investigation holds the promise of shedding valuable insights into how the choice of organic sulphur salt precursors can be effectively harnessed to fine-tune the morphology, size, and optoelectronic characteristics of CdS nanocrystals. Beyond its contributions to fundamental scientific knowledge, the outcomes of this research bear significant implications for a wide range of applications in nanotechnology, materials science, and related disciplines [28, 29]. As we embark on this exciting journey of exploration, we anticipate that our findings will pave the way for the development of innovative and tailored nanomaterials with enhanced functionalities and superior performance across a spectrum of technological domains [30, 31].

II. EXPERIMENTAL

A. Preparation of Sulphur Sources:

➤ *Thiocarbohydrazide TCH (l)*

The 250 ml round bottom flask was filled with 150 ml of 99% aqueous hydrazine hydrate, and the temperature was decreased to 10°C. Dropwise additions of 50 mL of carbon disulphide were made during the course of about 30 minutes of stirring at a temperature below 15°C. The reaction mixture was allowed to settle at room temperature for 30 minutes. The resulting thick mixture was then heated under reflux to 70° C for 25 hours using mental heater. After cooling, the reaction mixture was filtered off, washed with benzene, dried and then crystallized with hot water contains drops of hydrochloric acid to give white needles in 93% yield; m.p= 170 ºC; IR (KBr): ν 3350-3204 cm^{-1} (NH and NH$_2$), 1286 cm^{-1} (C=S); ^{1}H-NMR (*DMSO-d$_6$*, 400 MHz): δ 9.2 (NH, 2H), δ 4.49, (NH$_2$, 4H); MS: m/z=106 m/z (100%) for CH_6N_4S.

➤ *Synthesis of Thiocarbonic Acid Dipotassium Salt (ll):*

A mixture of potassium sulphide (11 gm, 0.1 mol) and carbon disulphide (6 ml, 0.1 mol) in 40 ml distilled water was stirred at room temperature for 24 hours. The heavy red syrup formed was left to stand for few days till dryness. The solid formed was used directly without further purification: 81% yield; Chars without melting at 280 ºC; IR (KBr): ν 1132 cm^{-1} (C=S); MS: 126 (0.93 %) for CS_2K_2.

➤ *Synthesis of Thiocarbonyl-Bis-Thioglycolic Acid (lll):*

Compound III was prepared from the salt II according to the literature method [32,33]. To the red syrup of the salt II, simultaneously a solution of chloroacetic acid potassium salt (13.2 gm, 0.1 mol) in 100 ml of dist. water (After neutralization of 9.4 gm by 10 gm of KHCO$_3$) has been added dropwise. The resulting solution has been further stirred for 1 hour and let to stand. After 24 hours the reaction mixture was acidified by concentrated HCl to the PH= 3. The resulted precipitate has been filtered off and crystallized by hot water to give yellow needles in 88% yield; m.p= 150 ºC; IR (KBr): ν 3452 cm^{-1} (Carboxylic-OH), 2919 (CH-aliphatic), 1700 cm^{-1} (C=O), 1346 cm^{-1} (C=S); ^{1}H-NMR (*DMSO-d$_6$*, 400 MHz): δ 12.87 ppm (carboxylic (OH, 2H), δ 4.27 ppm (2CH$_2$, 4H); MS: m/z=226 (3.33 %) for $C_5H_6O_4S_3$.

B. Synthesis of CdS nanoparticles

➤ *General Procedure:*

A solution of Cd (NO$_3$).4H$_2$O (1.54, 0.005 mol) in warm Ethanol (100 ml) was gradually added to solution of thiocarbohydrazide, thiocarbonic acid dipotassium salt and/or thiocarbonyl-Bis-thioglycolic acid (0.01 M) in hot water (100 ml) with constant stirring for 30 minutes, 10 ml of aqueous solution of potassium hydroxide (0.7 g, 0.0125 M) was added with stirring to the reaction mixture. A white precipitate was formed at first, which turns to yellow precipitate of CdS by heating under reflux for 3 hours. The solid formed was filtered off on hot, washed with hot distilled water and dried at 100ºC to give CdS (**I**), CdS (**II**) and/or CdS (**III**) respectively.

C. Characterizations

High purity chemicals are the starting materials utilized to create CdS nanocrystalls. An FT-IR 8101 PC spectrometer from Shimadzu was used to record the IR spectra. The 300 MHz Varian Mercury VX 300 NMR spectrometer and the AVANCE-III 400 MHz High-Performance FT-NMR Spectrum BRUKER, both manufactured by BioSpen International AG in Switzerland, were used to determine the 1H-NMR spectra in DMSO-d6. Tetramethylsilane is used as an internal standard, and chemical changes are reported in parts per million and expressed in units. A GCMS-QP 1000 EX spectrometer was used to produce electron impact mass spectra at 70 eV. X-ray powder diffraction (XRD), using a PANalytical diffractometer with a Cu target and a graphite monochromator (λ=1.54056 Å), was used to determine the phase purity and structure of the prepared samples. High resolution transmission electron microscopy (HRTEM) images were captured using a JEOL JEM 2100 microscope (Japan). An energy dispersive x-ray analysis (EDX) spectrometer (Elemental Analyzer EDXRF, JSX3222, JEOL, Japan) connected to a scanning electron microscope was used to identify the chemical composition of the materials. A computerized double beam SPECORD 200 PLUS spectrophotometer (Germany) was used to measure the UV-visible absorption spectra in the wavelength range of 200-1100 nm at normal incidence at room temperature.

III. RESULTS AND DISCUSSION

In conjunction of our previous works in the preparation of metal sulphides nanoparticles [32,33], present a comparison study in the synthesis of cadmium sulphide nanoparticles between three different organic sulphur sources such as Thiocarbohydrazide (**I**), thiocarbonic acid dipotassium salt (**II**) and thiocarbonyl-bis-thioglycolic acid (**III**) using simple chemical reaction in basic medium.

So, boiling of any of the above sulphur sources **I, II** and **III** in equivalent amount of ethanol/ water with Cd(NO$_3$).4H$_2$O will produce three different CdS (**I, II** and **III**) nanoparticles in there characterizations. (**Scheme 1**)
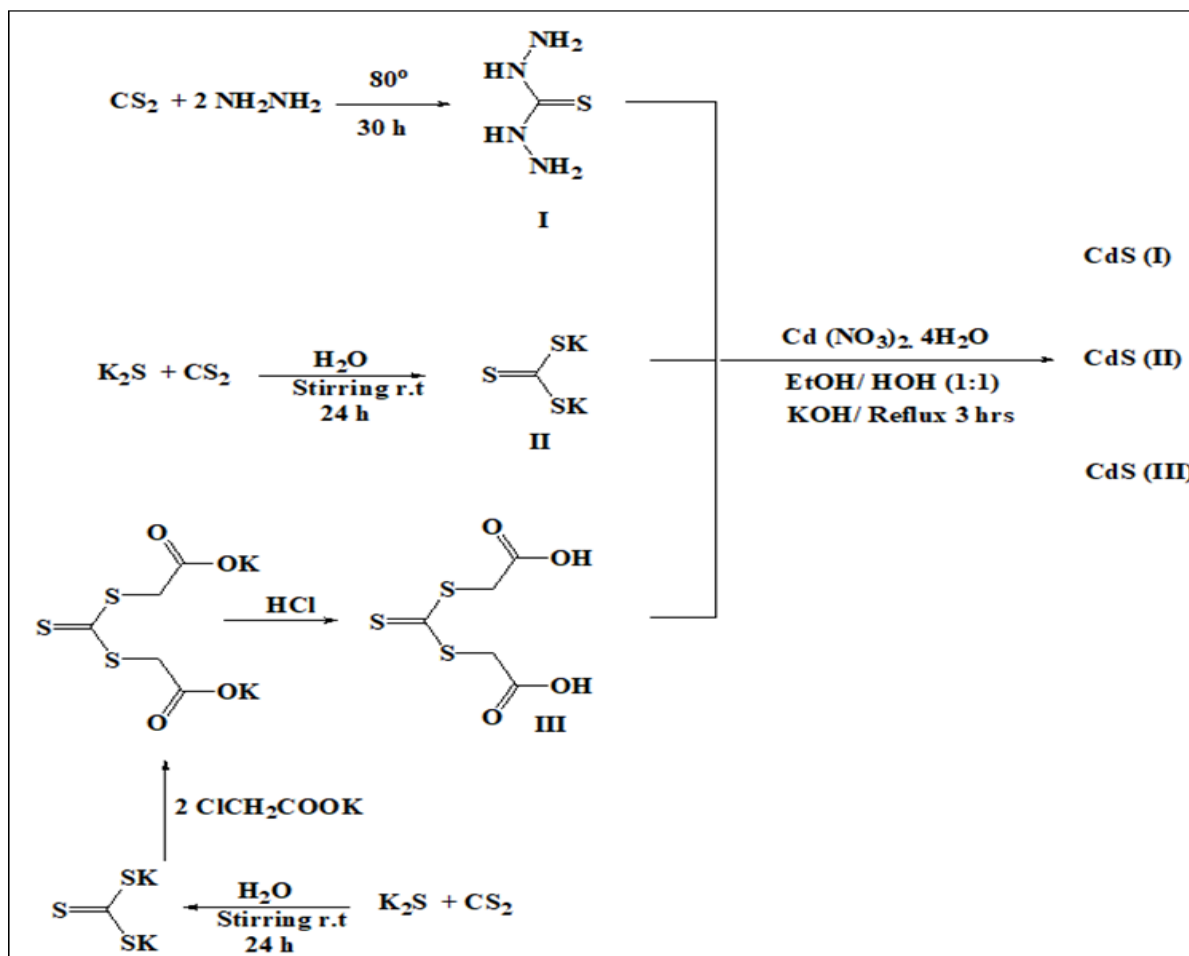
Scheme 1

The chemical structure of all the prepared sulphur sources was characterized by FT-IR, ^{1}H NMR, and MS spectra as shown in the experimental part. The mass spectra of the used sulphur sources are shown in **Figures 1, 2** and **3**.
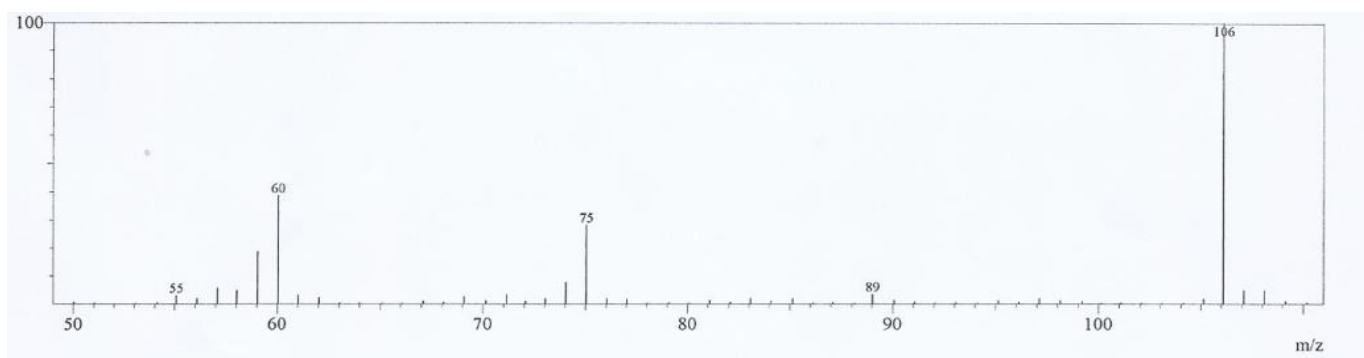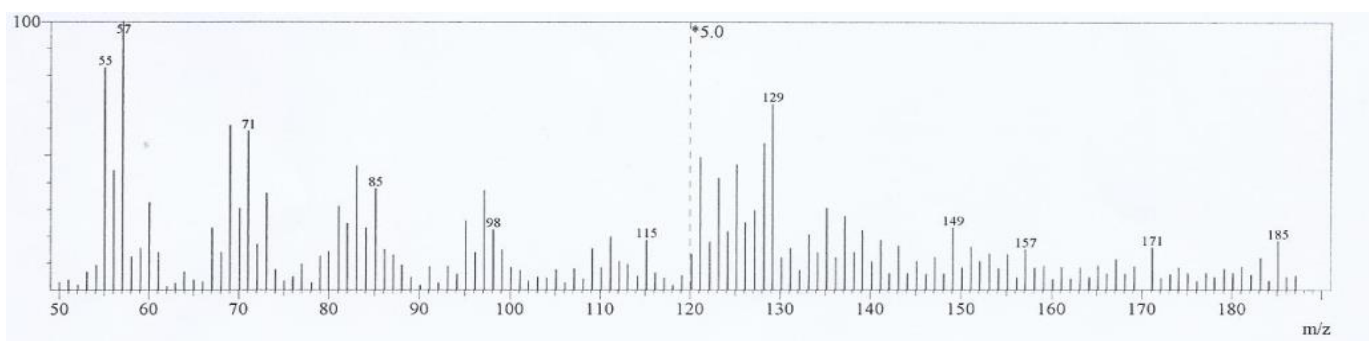

Fig 1 The Mass Spectrum of TCH

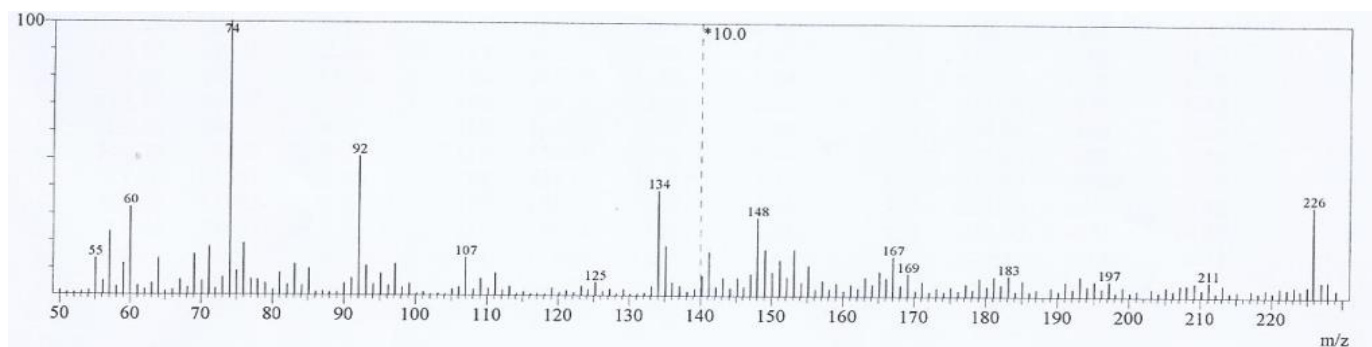Fig 2 The Mass Spectrum of Thiocarbonic Acid Dipotassium Salt

Fig 3 The Mass Spectrum of Thiocarbonyl-Bis-Thioglycolic Acid

A. X-ray Analysis

In conjunction of our previous works in the preparation of metal sulphides nanoparticles, the prepared CdS samples from the three different sulphur sources were investigated using XRD analysis. The spectra confirm the crystalline nature of the prepared samples. For the first sample CdS(I), the spectrum was characterized by eight mean peaks (100), (002), (101), (102), (110), (103), (112) and (300) which refer to hexagonal CdS phase [34], while the spectra for CdS(II) and CdS (III) samples were defined by the Cubic CdS phase's three average peaks (111), (220), and (222) [35] .
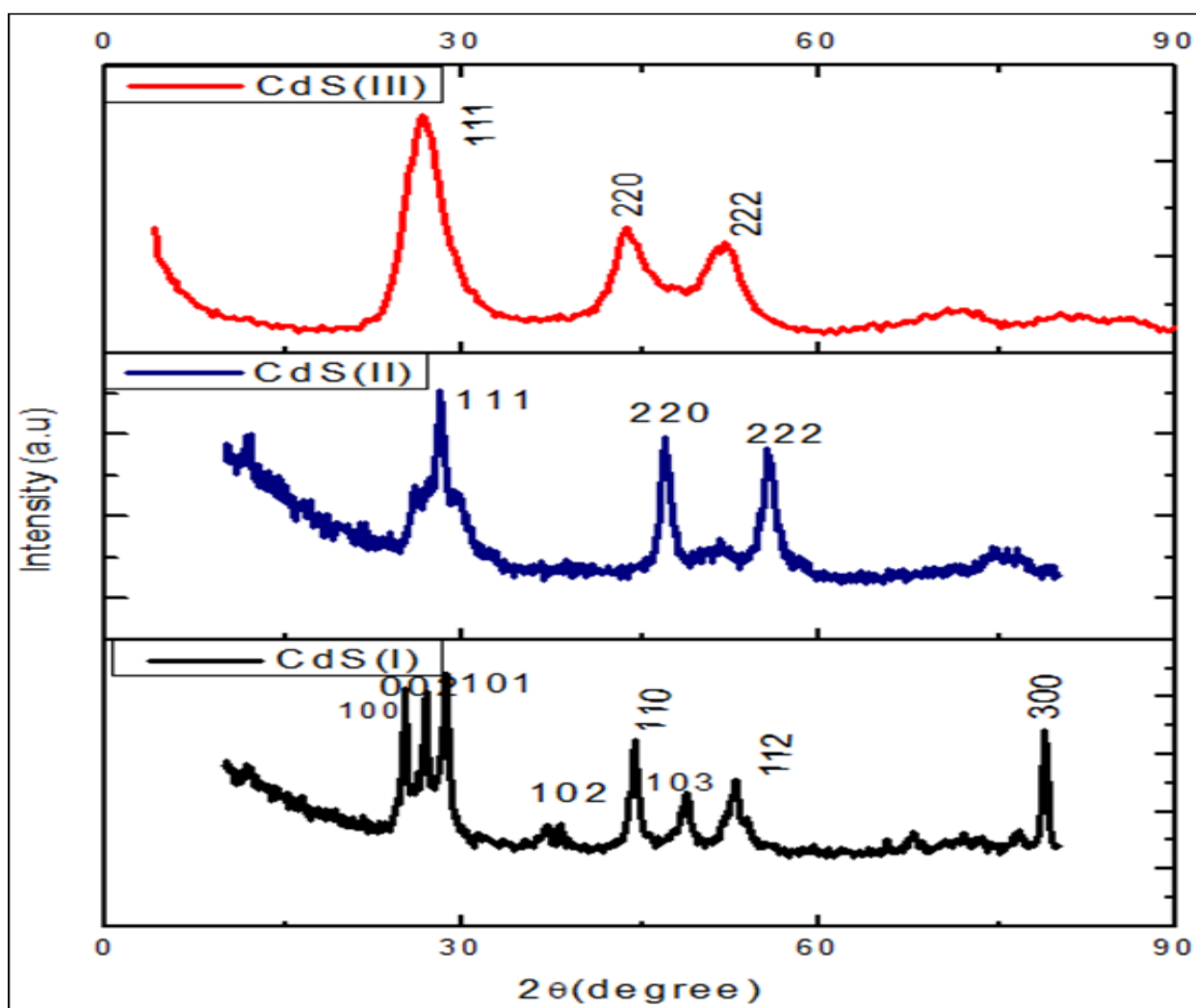

Fig 4 XRD of CdS NPs

➢ Calculation of Lattice Parameters

Figure 5 displays the variation of lattice parameters with the angular function F(θ) for the grown samples. According to the data in the Figure, the lattice parameters for the CdS (I) nanoparticles that were obtained are a = b = 4.086Å and c = 6.618Å. In contrast, for CdS (II) and CdS (III), the lattice parameters are a = 5.5Å and 5.79Å, respectively. These determined lattice parameters align with the standard lattice parameters of hexagonal and cubic CdS crystals [34,35].
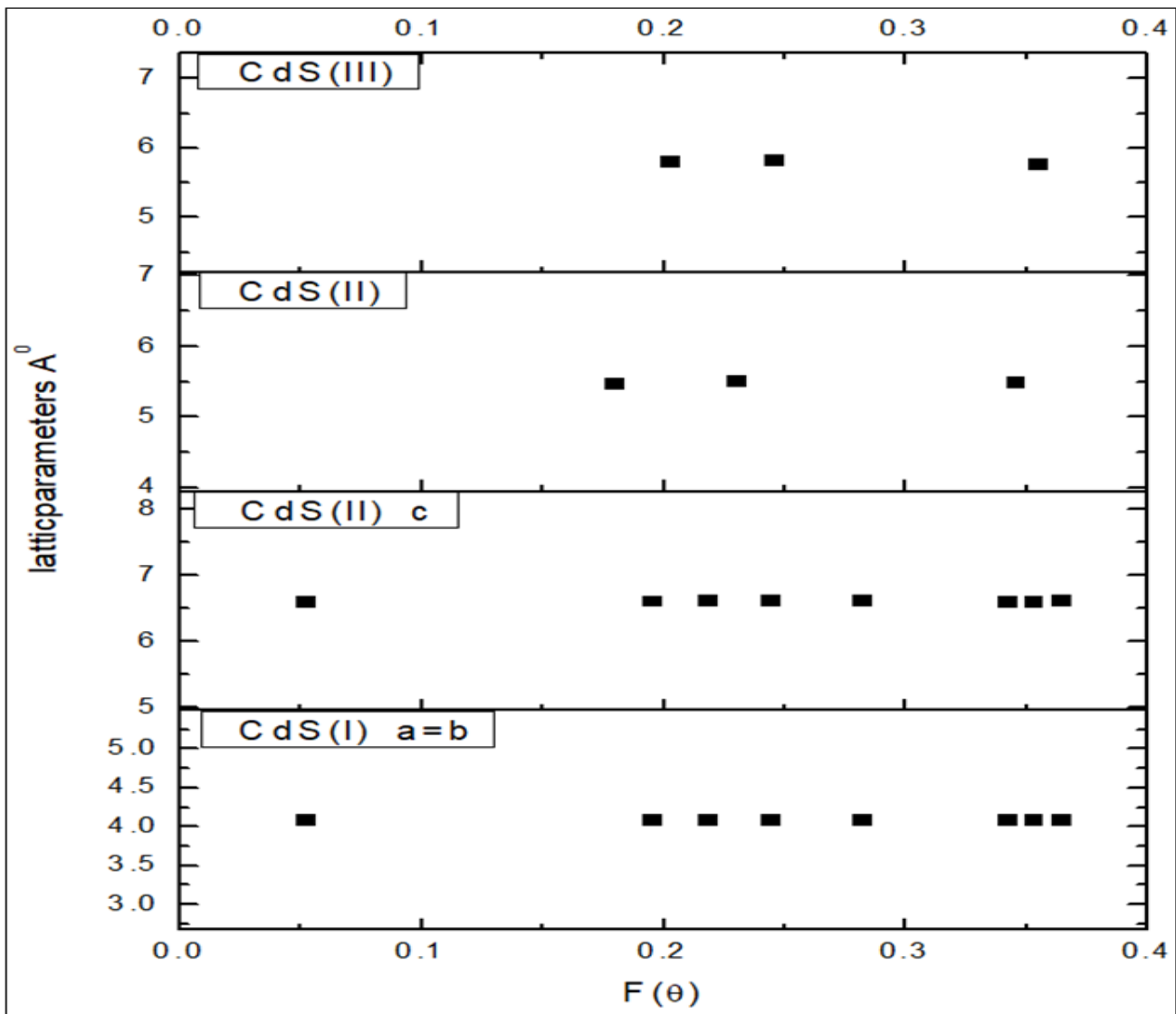
Fig 5 Lattice Parameters for CdS NPs

> *Crystallite Size and Microstrain*

The generated CdS nanoparticles' crystallite size (D) can be calculated using the Debye-Scherrer equation [36]:

$$D = \frac{nK\lambda}{\beta cos\theta}$$ …………………………………………..(1)

λ represents the wavelength of the X-ray radiation, D stands for the size of the crystalline particles, θ denotes the incident angle (the angle formed between the incident ray and the scatter plane), n is an integer, β signifies the full width at half maximum of the diffraction peak measured at 2θ, and K is the Sherrer constant. The average crystallite size of the CdS nanoparticles that were synthesized was determined using Debye-Scherrer's equation [37], resulting in values of 22.56, 12.706, and 4.65 for the respective samples CdS (I), CdS (II), and CdS (III). Table (1) summarized the obtained values.

The size of the crystalline particles (D) and the level of microstrain (ε) in the nanoparticles can be determined by analyzing the X-ray diffraction (XRD) patterns through the Williamson-Hall method. The Williamson-Hall equation

accounts for the overall broadening of the diffraction peaks, involving two distinct factors: the first factor relates to the size of the crystalline particles (D), while the second factor represents the impact of strain (ε).

$$\beta = \beta_D + \beta_\varepsilon$$ ....(2)

The Williamson-Hall equation can be expressed as follows [38]:

$$\beta \, cos\theta = \frac{0.94 \, \lambda}{D} + 4 \, \varepsilon \, sin\theta$$ …………………….………...(3)

The size broadening (β_D) is proportional to $cos^{-1}\theta$ and the strain broadening (β_ε) is proportional to tanθ.

To calculate the crystallite size and the microstrain of the CdS nanoparticles, a relationship between β cosθ/λ and sinθ/λ is drawn for the prepared samples and is shown in **Figure 6**. The average crystallite size of CdS nanoparticles is 20.76, 20.18 and 24.76 nm, while its microstrain value are about 0.00084, 0.00266 and 0.0174 for the prepared samples CdS (I), CdS (II) and CdS (III) respectively.
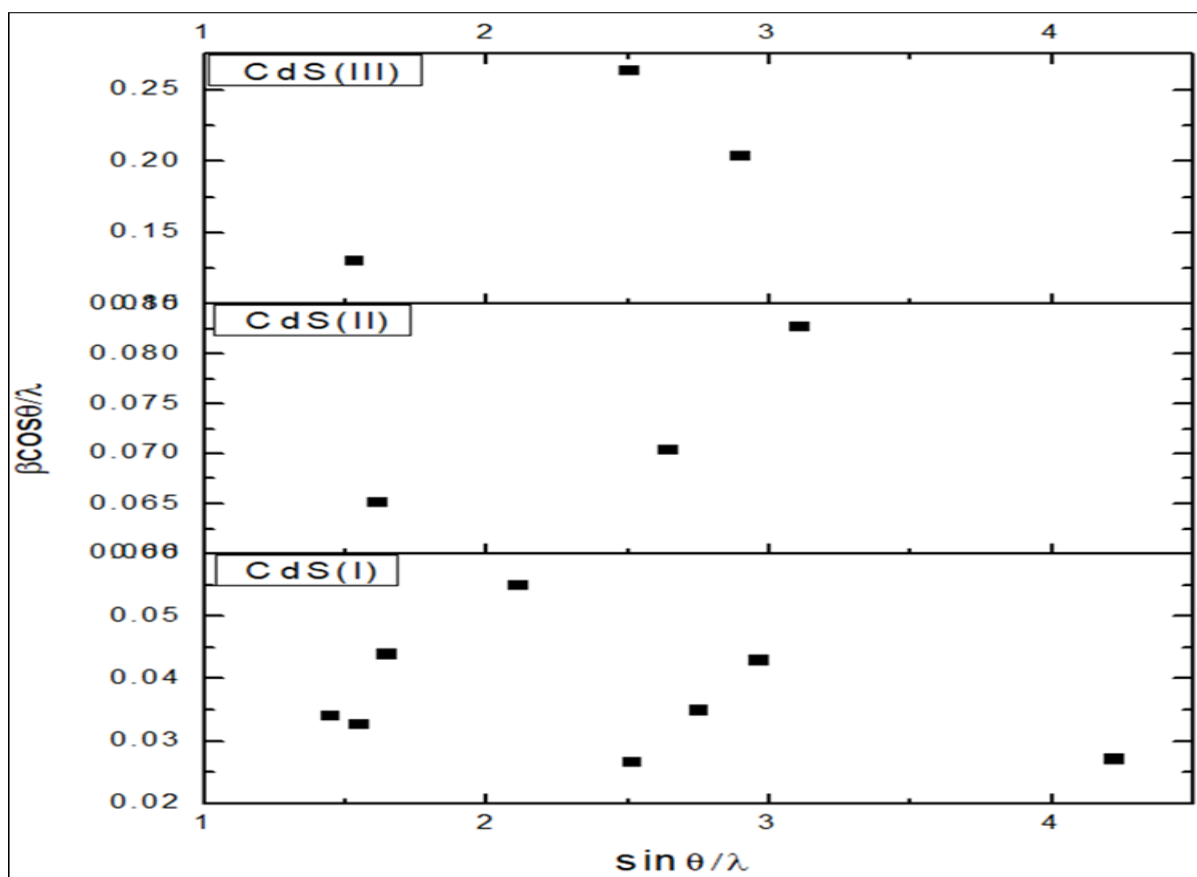
Fig 6 Williamson- Hall Plot for CdS NPs

Table 1 Size and Lattices Parameters of CdS NPs

Sample	Lattice Parameters measured (Å)		Crystal size (nm)		Microstrain x10-3
	a=b	C	Scherrer	Williamson – Hall	
CdS(I)	4.086	6.618	22.56	20.76	0.00084
CdS(II)	5.5	5.5	12.706	20.18	0.00266
CdS(III)	5.79	5.79	3.18	24.76	0.0174

B. FTIR of CdS nanoparticles

FTIR is employed for examining the composition of the produced materials and identifying the functional groups and bond types within the system. The FT-IR spectra of the three CdS nanoparticle samples revealed distinct broad absorption bands in the range of (3414 – 3376) cm^{-1}, which can be attributed to lattice water (OH group). [39] due to the presence of small amount of water adsorbed on the samples. The absorption bands located at 604 - 616 cm^{-1} is due to S-S bond (crystal s-s bond) [40], which are broad in CdS (II) and CdS (III), and the bands between 423– 473 cm^{-1} are signify to the existence of Cd-S bond (CdS nanoparticles) [41]. Strong bands position at ~1580 cm^{-1} is possibly due to stretching vibrations of the sulphate group. As shown in **Figure 7**, the FTIR results indicate the fabrication of pure CdS and Cds (III) samples.
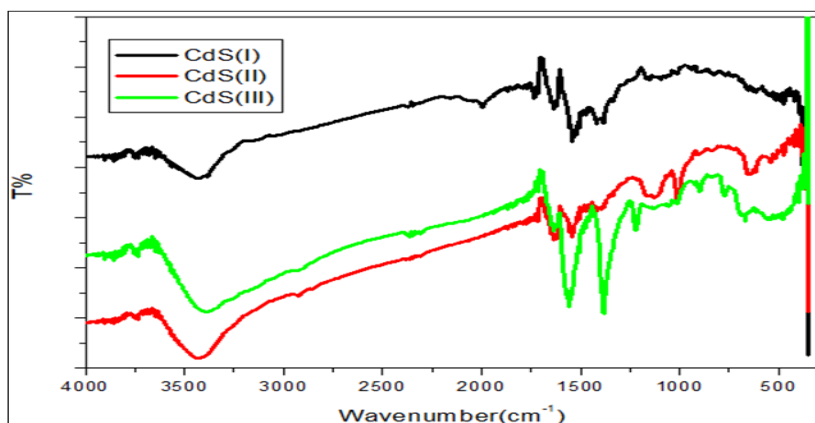

Fig 7 FTIR of CdS NPs
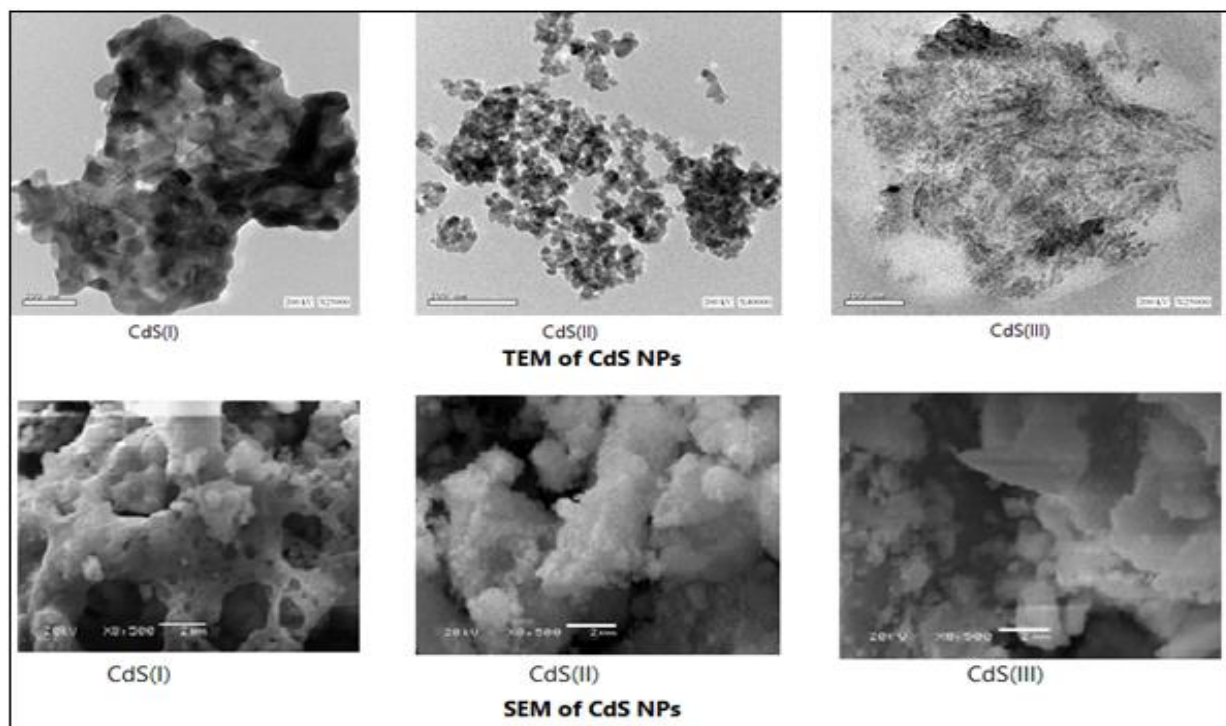
C. Morphology of CdS nanoparticles

Fig 8 Morphology of CdS NPs

Figure 8 displays the SEM and HRTEM images of the CdS samples that were prepared. As shown from the Figure, the used sulfur source affects the morphology and the size of the obtained CdS samples. The HRTEM results confirm XRD data, where CdS (I) has particle size higher than that for CdS(II) and CdS(III).

D. EDX of CdS NPs:-

Table 2 The Ratio Cd: S in Obtained CdS N

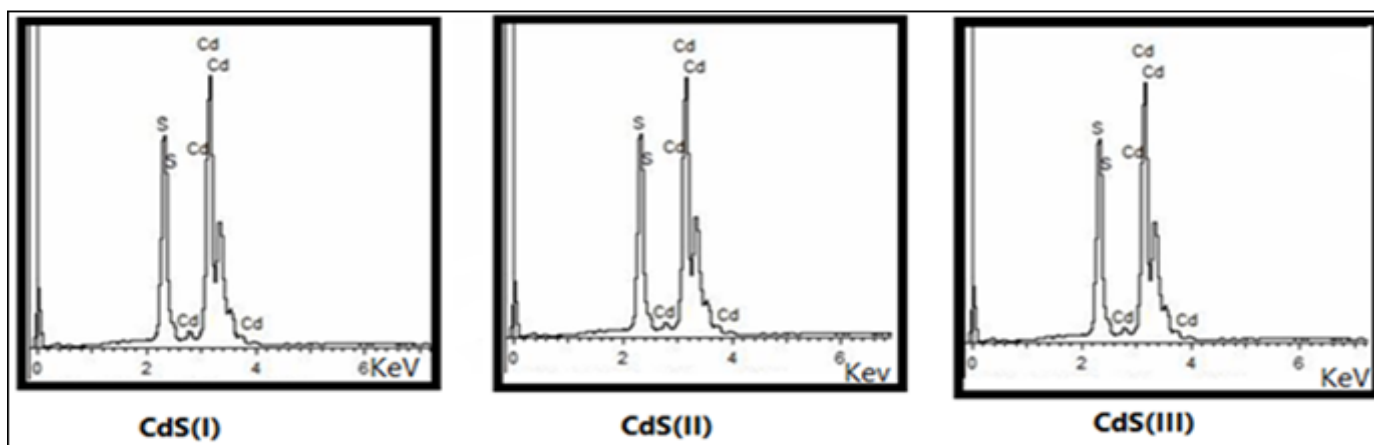| Sample	Cd%	S%
CdS(I)	78.36	21.64
CdS(II)	75.13	24.87
CdS(III)	74.25	25.75
Stoichiometry (Cd:S)	77.848	22.196

Fig 9 EDX of CdS NPs

Figure 9 depicts the EDX spectra of CdS nanoparticles sourced from various sulfur sources, revealing the presence of both Cd and S elements. It is noteworthy that there are no extra peaks corresponding to impurities or contaminants, confirming the purity of the obtained samples. The ratio of Cd to S varies when different sulfur sources are used. As indicated in table (2), the CdS(I) sample is the one that most closely approximates the stoichiometric ratio of Cd to S.
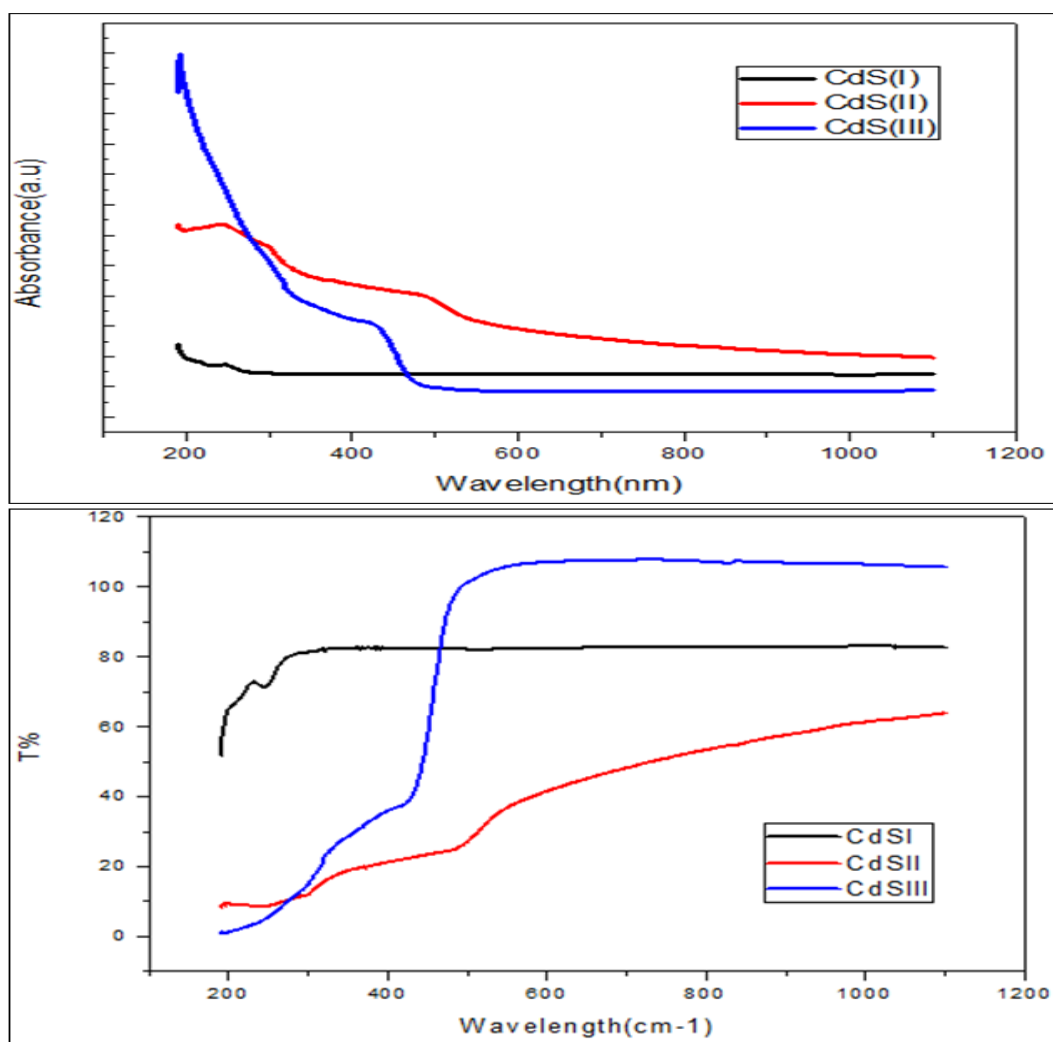
E. Optical Properties of CdS nanoparticles

Fig 10 Absorbance and Transmittance Spectra of CdS NPs

Absorbance and transmittance measurements were conducted at nearly perpendicular incidence angles, covering a spectral range from 200 to 1100 nm. While the shapes of the curves were comparable, variations in absorption and transmission were observed. The using thiocarbonyl bis-thioglycolic acid as sulphur salt led to get the highest absorbance between the prepared samples, while using thiocarbonhydrizide as sulphur salt gives CdS sample has the highest transmittance between the prepared samples.
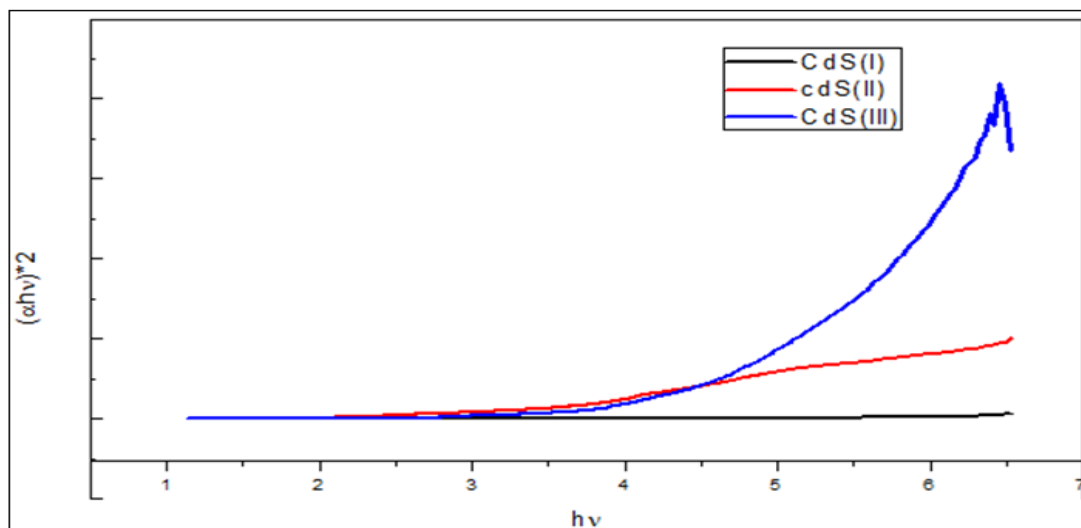

Fig 11 The Relationship between $(\alpha h\nu)^2$ and $h\nu$ for the Produced CdS NPs

Table 3 Energy Band Gap of CdS NPs

Samples	CdS(I)	CdS(II)	CdS(III)	Bulk CdS
Energy band gap (eV)	4.87	3.22	5.03	2.42

The direct optical band gap, associated with a direct transition, can be determined using the following formula [42]:

$$\alpha h\nu = B\,(h\nu - E_g)^{1/2},\ldots\ldots\ldots\ldots\ldots\ldots\ldots\ldots\ldots\,(4)$$

Where $h\nu$ is the energy of the photon, B is a constant influenced by the likelihood of the transition, α stands for the absorption coefficient, and E_g signifies the optical band gap. From the **Figure 14** the values of E_g are 4.87, 3.22 and 5.03 eV for CdS(I), CdS(II) and CdS(III) respectively.

The effective mass model [43] used to calculate the particles radius according to:

$$\Delta E_g = E_{g\,nano} - E_{g\,bulk} = h^2/\,8M\pi r^2\ldots\ldots\ldots\ldots\ldots\ldots\ldots\ldots(5)$$

Where r is the radius of the particle, m_e is the effective mass of the electrons, m_h is the effective mass of the holes, m_0 is the free electron mass, e is the relative permittivity, ε_o is the permittivity of free space, h is the reduced Planck's constant and e is the electron charge.

The characteristics of nanocrystalline materials deviate from their bulk counterparts when the size of the crystallites becomes comparable to the Bohr excitonic radius (r_B) [44].

$$r_B = h^2\varepsilon[1/m_e^* + 1/m_h^*]/\pi e^2\ldots\ldots\ldots\ldots\ldots\ldots\ldots\ldots(6)$$

Where ε is the permittivity of the sample, $m_e^* = 0.21\,m_o$ and $m_h = 0.80\,m_o$ are the effective mass of electron and hole in CdS, respectively, where m_o is the mass of a free electron. From the above relation the Bohr radius of CdS has been calculated to be 2.8 nm [44, 45].

The values of particles radius are 2.66, 3.9 and 2.41 nm for CdS(I), CdS(II) and CdS(III) respectively.

From the previous, show that the obtained CdS nanoparticles are confined, and the band gap increasing with decreasing particle redius.

IV. CONCLUSION

In summary, the structural properties of CdS nanoparticles were significantly influenced by the choice of the organic sulphur source employed in the synthesis process. Specifically, the utilization of thiocarbohydrazide as a sulphur source resulted in the preparation of hexagonal-phase CdS nanoparticles, whereas the usage of thiocarbonic acid dipotassium salt and thiocarbonyl-bis-thioglycolic acids as sulphur sources yielded cubic-phase CdS nanoparticles.

Moreover, our investigation revealed a notable impact of the selected sulphur source on the particle size of the prepared CdS nanoparticles. Thiocarbohydrazide yielded CdS nanoparticles with a particle size of 22.56 nm, while thiocarbonic acid dipotassium salt produced CdS nanoparticles with a reduced particle size of 12.7 nm. Remarkably, the utilization of thiocarbonyl-bis-thioglycolic acids as the sulphur source resulted in the smallest particle size observed, with CdS nanoparticles measuring only 3.18 nm in diameter.

Furthermore, the optical band gap of the prepared CdS NPs exhibited sensitivity to the choice of the organic sulphur source. Specifically, CdS NPs synthesized with thiocarbohydrazide exhibited an optical band gap of 4.87 eV, whereas those derived from thiocarbonic acid dipotassium salt displayed a reduced band gap of 3.22 eV. Remarkably, the utilization of thiocarbonyl-bis-thioglycolic acid as the sulphur source resulted in the widest band gap observed, measuring 5.03 eV for the prepared CdS nanoparticles. This variation can be attributed to the pronounced reduction in particle size induced using thiocarbonyl-bis-thioglycolic acid.

Importantly, our findings underscore the role of the sulphur source in tailoring the structural and optical properties of CdS nanoparticles, highlighting the potential for fine-tuning nanoparticle characteristics through rational selection of precursor materials. Furthermore, the purity of the synthesized CdS samples was confirmed through FT-IR and EDX analysis, validating the integrity of the prepared nanocrystals.

In conclusion, this study provides valuable insights into the versatile influence of organic sulphur sources on the synthesis and characteristics of CdS nanoparticles, offering a foundation for further exploration and application of these nanomaterials in diverse scientific and technological domains.

REFERENCES

[1]. Bhattacharya, R., & Saha, S. (2008). Growth of CdS nanoparticles by chemical method and its characterization. Pramana, 71(1), 187-192.

[2]. Dumbrava, A., Badea, C., Prodan, G., & Ciupina, V. (2010). Synthesis and characterization of cadmium sulfide obtained at room temperature. Chalcogenide Lett, 7(2), 111-118.

[3]. Banerjee, R., Jayakrishnan, R., & Ayyub, P. (2000). Effect of the size-induced structural transformation on the band gap in CdS nanoparticles. Journal of Physics: Condensed Matter, 12(50), 10647.

[4]. Abdellah, I. M., Eletmany, M. R., & El-Shafei, A. (2023). *Exploring the impact of electron acceptor tuning in D-π-A'-π-A photosensitizers on the photovoltaic performance of acridine-based DSSCs: A DFT/TDDFT perspective*. Materials Today Communications, 35, 106170.

[5]. Eletmany, M. R., Aziz Albalawi, M., Alharbi, R. A. K., Elamary, R. B., Harb, A. E.-F. A., Selim, M. A., … Abdellah, I. M. (2023). *Novel arylazo nicotinate derivatives as effective antibacterial agents: Green synthesis, molecular modeling, and structure-activity relationship studies*. Journal of Saudi Chemical Society, 27(3), 101647.

[6]. Barqi, M. M., Abdellah, I. M., Eletmany, M. R., Ali, N. M., Elhenawy, A. A., & Abd El Latif, F. M. (2023). *Synthesis, Characterization, Bioactivity Screening and Computational Studies of Diphenyl−malonohydrazides and Pyridines Derivatives*. ChemistrySelect, 8(2).

[7]. Eletmany, M. R. (2019). *Development of New Organic Hole Transport Compounds for high Performances Organic Solar cells*. 3rd International Conference on Natural Resources and Renewable Energy (ICNRRE). Presented at the 3rd International Conference on Natural Resources and Renewable Energy (ICNRRE), South Valley University, Hurghada, Egypt.

[8]. Liu, L. W., Hu, S. Y., Pan, Y., Zhang, J. Q., Feng, Y. S., & Zhang, X. H. (2014). Optimizing the synthesis of CdS/ZnS core/shell semiconductor nanocrystals for bioimaging applications. Beilstein journal of nanotechnology, 5(1), 919-926.

[9]. Li, Q., & Penner, R. M. (2005). Photoconductive cadmium sulfide hemicylindrical shell nanowire ensembles. Nano Letters, 5(9), 1720-1725.

[10]. Eletmany, M. R., Hassan, E. A., Fandy, R. F., & Aly, K. I. (2019). *Synthesis and Characterization of Some New Benzoxazine Polymers with Their Industrial Applications. 3rd Annual Conference of the Faculty of Science*. Presented at the 3rd Annual Conference of the Faculty of Science, Faculty of Science, South Valley University, Qena, Egypt.

[11]. Eletmany, M. R., Hassan, E. A., Fandy, R. F., & Aly, K. I. (2019). *Synthesis and characterization of Novel 2-substituted 1,3-benzoxazines monomers and studies their Polymerization*. 14th International Conference on Chemistry and its Role in Development (ICCRD-2019). Presented at the 14th International Conference on Chemistry and its Role in Development (ICCRD-2019), Mansoura University, Hurghada, Egypt.

[12]. Aly, K. I., Fandy, R. F., Hassan, E. A., & Eletmany, M. R. (2018). *Synthesis and characterization of novel 1,3- benzoxazines monomers and studies their polymerization and industrial applications*. Assiut University 11th International Pharmaceutical Sciences Conference. Presented at the Assiut University 11th International Pharmaceutical Sciences Conference, Faculty of Pharmacy, Assiut, Egypt.

[13]. Fang, Y. M., Song, J., Zheng, R. J., Zeng, Y. M., & Sun, J. J. (2011). Electrogenerated chemiluminescence emissions from CdS nanoparticles for probing of surface oxidation. The Journal of Physical Chemistry C, 115(18), 9117-9121.

[14]. 14-Demir, R., Okur, S., & Şeker, M. (2012). Electrical characterization of CdS nanoparticles for humidity sensing applications. Industrial & Engineering Chemistry Research, 51(8), 3309-3313.

[15]. Shang, L., Tong, B., Yu, H., Waterhouse, G. I., Zhou, C., Zhao, Y., & Zhang, T. (2016). CdS nanoparticle-decorated Cd nanosheets for efficient visible light-driven photocatalytic hydrogen evolution. Advanced Energy Materials, 6(3), 1501241.

[16]. Ashar, A., Bhutta, Z. A., Shoaib, M., Alharbi, N. K., Fakhar-e-Alam, M., Atif, M., … Ezzat Ahmed, A. (2023). Cotton fabric loaded with ZnO nanoflowers as a photocatalytic reactor with promising antibacterial activity against pathogenic E. coli. Arabian Journal of Chemistry, 16(9), 105084.

[17]. Abo-Bakr, A. M., Salman, H. M., Ismael, E. M., Ebnalwaled, K. (2020). Thiocarbohydrazide as a Sulfur Source for the Preparation of Nickel Sulfide Nanoparticles. J. Pharm. Appl. Chem., 6, No. 2, 41-45.

[18]. Ristić, M., Popović, S., Ivanda, M., & Musić, S. (2013). A simple route in the synthesis of CdS nanoparticles. Materials letters, 109, 179-181.

[19]. Selim, M. A., Hassan, E. A., Harb, A.-E. A., & Eletmany, M. R. (2016). *Some spectral studies of New Derivatives of Nicotine, Pyridazine, Cinnoline Compounds*. 7th International Conference on Optical Spectroscopy, Laser and Their Applications. Presented at the 7th International Conference on Optical Spectroscopy, Laser and Their Applications, NRC, Cairo, Egypt.

[20]. Selim, M. A., Hassan, E. A., Harb, A.-E. A., & Eletmany, M. R. (2015). *Synthesis of Some New Derivatives of Nicotine via the Reaction of Arylhydrazonals with Active Methylene Derivatives*. 13th IBN SINA International Conference on Pure and Applied Heterocyclic Chemistry. Presented at the 13th IBN SINA International Conference on Pure and Applied Heterocyclic Chemistry, Hurghada, Egypt.

[21]. Eletmany, M. R., Hassan, E. A., Harb, A. E.-F. A., & Selim, M. A. (2017). *Reaction of 3-Oxo-arylhydrazonal derivatives with active methylene nitriles*. London: LAMPERT Academic Publishing. https://www.worldcat.org/isbn/9783330328730

[22]. Ashar, A., Qayyum, A., Bhatti, I. A., Aziz, H., Bhutta, Z. A., Abdel-Maksoud, M. A., Saleem, M. H. and Eletmany, M. R. (2023). *Photo-Induced Super-Hydrophilicity of Nano-Calcite @ Polyester Fabric: Enhanced Solar Photocatalytic Activity against Imidacloprid*. ACS Omega, https://doi.org/10.1021/acsomega.3c02987

[23]. Mahmood, N., Eletmany, M. R., Jahan, U. M., El-Shafei, A., Gluck, J. M. (2323). *Surface Modified Fibrous Scaffold for Ocular Surface Regeneration*, Society for Biomaterials: 2023 Annual Meeting and Exposition, San Diego, California

[24]. Eletmany, M. R., El-Shafei, A (2023). *Cotton Dyeing for Sustainability and Long-Lasting Color Fastness using Reactive dyes*, 2022-2023 Research Open House Conference - Duke Energy Hall, Hunt Library, NC State University, North Carolina, USA. http://dx.doi.org/10.13140/RG.2.2.14979.68642

[25]. Abdel Aziz, E. M., Elmorshedy, H. A., Abd-Elkader, A. S., Haridi, Mostafa A. (2022). *Causes of End Stage Renal Disease in patients undergoing regular hemodialysis in Assiut University Hospital*, Sapporo igaku zasshi. The Sapporo medical journal 55(12):12.

[26]. BEGGAS, A. (2018). Elaboration and characterization of chalcogenide thin films by chemical bath deposition technique (Doctoral dissertation, UNIVERSITE Mohamed Khider Biskra).

[27]. Yang, D., Xu, S., Chen, Q., & Wang, W. (2007). A simple organic synthesis for CdS and Se-doped CdS nanocrystals. Colloids and Surfaces A: Physicochemical and Engineering Aspects, 299(1-3), 153-159.

[28]. Billakanti, S., & Krishnamurthi, M. (2018). Facile preparation of surfactant or support material free CdS nanoparticles with enhanced photocatalytic activity. Journal of environmental chemical engineering, 6(1), 1250-1256.

[29]. Lahewil, A. S., Al-Douri, Y., Hashim, U., & Ahmed, N. M. (2013). Structural, analysis and optical studies of cadmium sulfide nanostructured. Procedia engineering, 53, 217-224.

[30]. Kotkata, M. F., Masoud, A. E., Mohamed, M. B., & Mahmoud, E. A. (2009). Synthesis and structural characterization of CdS nanoparticles. Physica E: Low-dimensional Systems and Nanostructures, 41(8), 1457-1465.

[31]. Khaled Ebnalwaled, Ahmed A. Abd El-Raady, Ahmed M. Abo-Bakr; On the effect of complexing agents on the structural and optical properties of CdS nanocrystals; Chalcogenide Letters. 10, 2, 55 – 62, 2013.

[32]. Ahmed M. Abo-Bakr, Ahmed A. Abd El-Raady, Khaled Ebnalwaled; Characterization of CdS nanocrystals grown from newly organic salt; IJSER "International Journal of Scientific & Engineering Research". 4, 11, 1349- 355, 2013.

[33]. Nektegayev, I., & Lesyk, R. (2000). 3-Oxyaryl-2-thionethiazolidones-4 and Their Choleretic Activity. ChemInform, 31(10), no-no.

[34]. F.Ulrich & W.H.Zachariasen, Z. Kristallogr., Kristallgeom., Kristallphys., Kristallchem., A62, 260, (1925)

[35]. Osugi, J., Shimizu, K., Nakamura, T., & Onodera, A. (1967). High pressure transition in cadmium sulfide.

[36]. Scherrer, P. (1912). Bestimmung der inneren Struktur und der Größe von Kolloidteilchen mittels Röntgenstrahlen. In Kolloidchemie Ein Lehrbuch (pp. 387-409). Springer, Berlin, Heidelberg.

[37]. Abdellah, I. M., Eletmany, M. R., Abdelhamid, A. A., Alghamdi, H. S., Abdalla, A. N., Elhenawy, A. A., & Latif, F. M. A. E. (2023). One-Pot Synthesis of Novel Poly-Substituted 3-Cyanopyridines: Molecular Docking, Antimicrobial, Cytotoxicity, and DFT/TD-DFT Studies. Journal of Molecular Structure, 1289, 135864.

[38]. Yuan, X. (2011). Enhanced interfacial interaction for effective reinforcement of poly (vinyl alcohol) nanocomposites at low loading of graphene. Polymer bulletin, 67(9), 1785-1797.

[39]. Sellmann, D. (1971). K. Nakamoto: Infrared Spectra of Inorganic and Coordination Compounds. John Wiley & Sons. New York, London, Sydney, Toronto, 1970. 338 Seiten, zahlreiche Abbildungen und Tabellen. Preis: 140s. Berichte der Bunsengesellschaft für physikalische Chemie, 75(6), 603-604.

[40]. Martin, T. P., & Schaber, H. (1982). Matrix isolated II-VI molecules: sulfides of Mg, Ca, Sr, Zn and Cd. Spectrochimica Acta Part A: Molecular Spectroscopy, 38(6), 655-660.

[41]. Pankove, J. I. (1971). Optical processes in semiconductors Prentice-Hall. New Jersey, 92.

[42]. Chestnoy, N., Harris, T. D., Hull, R., & Brus, L. E. (1986). Luminescence and photophysics of cadmium sulfide semiconductor clusters: the nature of the emitting electronic state. The Journal of Physical Chemistry, 90(15), 3393-3399.

[43]. Yoffe, A. D. (2001). Semiconductor quantum dots and related systems: electronic, optical, luminescence and related properties of low dimensional systems. Advances in physics, 50(1), 1-208.

[44]. Ghosh, P. K., Maiti, U. N., & Chattopadhyay, K. K. (2006). Structural and optical characterization of CdS nanofibers synthesized by dc-sputtering technique. Materials Letters, 60(23), 2881-2885.

[45]. Abdellah, I. M., & El-Shafei, A. (2020). The molecular engineering, synthesis and photovoltaic studies of a novel highly efficient Ru(ii) complex incorporating a bulky TPA ancillary ligand for DSSCs: donor versus π-spacer effects. RSC Advances, 10(1), 610–619.